Parametric Channel Estimation for Pseudo-Random Tile-Allocation in Uplink OFDMA

M. R. Raghavendra, Eldar Lior, Srikrishna Bhashyam, and K. Giridhar

Abstract—We consider the uplink channel estimation of a multipath wireless channel used for orthogonal frequency division multiple access (OFDMA) transmission, where the uplink uses a pseudo-random "tile" allocation pattern. A tile is made of small number of physically adjacent data subcarriers along with a few embedded pilot subcarriers and an uplink sub-channel allocated to an user in OFDMA systems such as IEEE 802.16d/e wireless MAN consists of several such pseudo-randomly chosen tiles. While the embedded pilots enable intra-tile channel interpolation, such an estimation will have an error floor which degrades performance substantially for highly frequency selective channels. We propose a parametric channel estimation method applicable to such irregular and sparsely spaced pilots, that does not exhibit an error-floor over the nominal operating range of signal to noise ratios, even for highly selective channels. The proposed algorithm exploits the pilot structure in each tile in estimating the delay subspace corresponding to the parametric channel description. Although this algorithm is more computationally complex when compared to the intra-tile linear interpolator, it offers a greatly enhanced bit-error probability (BEP) performance with a significantly lower pilot overhead. The uncoded BEP expression for the proposed estimator are analytically derived. Simulation results provided compares the mean squared error performance of this parametric channel estimator with the Cramer–Rao bound and also illustrates the significantly improved BEP performance over the existing methods.

Index Terms—ESPRIT, IEEE 802.16d/e standard, OFDM, parametric channel estimation, sparse multipath channels.

I. INTRODUCTION

SUBCARRIER allocation schemes in orthogonal frequency division multiplexing (OFDM) transmission are becoming increasingly complex, due to the need for greater flexibility in the allocation of transmission resources. The increased flexibility is necessary for simultaneous satisfaction of competing transmission needs of various applications requiring different qualities of service [1], [2]. The complexity of such schemes is further increased with the employment of pseudo-random resource allocation techniques introduced to recent wireless standards (such as IEEE 802.16d/e wireless MAN standard [3]) in order to provide protection against frequency selective fading and co-channel interference [4], [5].

The downside of such complex allocation schemes is the increased difficulty in estimating the channel response: the irregular distribution of channel information (implicitly held by pilots) over the available bandwidth hinders the estimation of channel interpolators which can utilize all the pilots, and also makes it difficult to estimate certain statistical properties such as frequency-correlation for channel interpolation. The wireless standards (such as [3]) have resorted to supplying local channel information by embedding pilots in each chunk of allocated bandwidth. However, the local channel information, in the absence of more global channel information (such as frequency correlation) is limited in its performance. In fact, in highly selective multi-path fading channels such as the hilly terrain scenario [6], nonstatistical linear interpolation of the channel response at data locations will be very erroneous and ineffective.

The channel estimation techniques for uplink OFDMA proposed in [7]–[9] suffer from significant pilot overhead for large delay-spread channels, and hence cannot be applied to outdoor mobile OFDMA transmissions [7, sec. 7]. Recently, a tile/chunk-based channel estimation method is proposed for uplink OFDMA [10]. However, it assumes ideal channel frequency correlation information (multipath delay information) at the receiver and does not address the vital issue of how to obtain this information from the sparse and random embedded pilot allocation.

Previous research [12]–[15] has shown that parametric channel estimation can greatly reduce the channel estimation error in sparse wireless channels. For example, the channel estimation method proposed in [12] recursively estimates the multipath locations using GAIC (generalized Akaike information criterion). In [13] the most significant taps (MST) approach is used to estimate the channel tap positions. Sparsity estimation using matching pursuit algorithm has been proposed in [14] for OFDM systems. However, the techniques proposed in [12]–[14] require atleast L_{cp} (length of the cyclic prefix in terms of samples) number of pilots for multipath-delay estimation. In uplink channel estimation, the base-station needs to estimate/track channel response for each user and hence employing the above methods leads to large pilot overheads. The work in [15] has relied on the assumption of evenly spaced pilot locations in frequency domain to estimate channel sparsity information and fails in the presence of irregularly spaced pilots.

In this paper, we relax the restriction of equal spacing between pilots and propose parametric channel estimation with ir-

regular pilot distribution.[1] This is achieved by relying on the uplink tile structure which generates the shift invariance property in the signal space, enabling the usage of the ESPRIT (estimation of signal parameters via rotational invariance technique [22]) algorithm to estimate the channel multipath delays. By this method, we are able to estimate the location of the channel taps within a marginal error, and as a result, decrease the channel estimation error significantly. The minimum number of pilots required for proposed algorithm is twice the number of actual paths (as against the number of CP samples), and hence it significantly reduces the pilot overhead required for channel estimation. Here we consider uplink tile structure as given in IEEE 802.16d/e [3]. However, the proposed channel estimation algorithm is not specific to IEEE 802.16d/e and can be applied to any tile-based OFDM system. We also analytically derive the Cramer–Rao bound (CRB) for the channel mean squared error and uncoded-bit-error-probability expressions for the existing and proposed channel estimation techniques.

The rest of the paper is organized as follows. Section II introduces the channel model and the OFDMA system model. In Section III, the improved channel estimation algorithm is provided. Section IV deals with the bit-error-probability analysis of the proposed channel estimator assuming a zero-forcing detector. A discussion of sub-channel allocation and receive diversity on the convergence of the proposed algorithm is given in Section V. The performance of the proposed algorithm is evaluated by computer simulations and the results are provided in Section VI. Comparisons are also made with the analytical results while Section VII summarizes the main results of the paper.

A. Basic Notation

In this paper, bold face letters denote vectors or matrices; $(.)^T$, $(.)^*$ and $(.)^H$ denote transpose, complex conjugate, and Hermitian, respectively; $\mathbf{0}$ denotes the zero column vector with appropriate dimension unless its size mentioned; $\mathbf{e}_p$ denotes the column vector whose pth entry is 1 and other entries are 0; $\mathcal{S}\{\mathbf{X}\}$ denotes the span of the columns of matrix $\mathbf{X}$; $\lfloor x \rfloor$ denotes the floor while $\lceil x \rceil$ denotes the integer nearest to x, $\text{tr}\{\mathbf{X}\}$ is the trace of matrix $\mathbf{X}$; $\text{sinc}(x) = (\sin(x)/x)$; $\bigcup_{i=1}^{k} \mathbf{x}_i$ denotes the union of vectors $\mathbf{x}_1, \mathbf{x}_2, \ldots, \mathbf{x}_k$; $[x_1, x_2, \ldots, x_k]$ denotes the diagonal matrix with $x_1, x_2, \ldots, x_k$ on its diagonal; $\mathcal{B}\{\mathbf{x}_1, \mathbf{x}_2, \ldots, \mathbf{x}_k\}$ denotes the block diagonal matrix with vectors $\mathbf{x}_1, \mathbf{x}_2, \ldots, \mathbf{x}_k$ on its diagonal.

II. OFDMA SYSTEM MODEL

A. Channel Model

Consider an OFDMA system with M active users sharing a bandwidth of $B = (1/T)$ Hz (T is the sampling period) as shown in Fig. 1. The system consists of K subcarriers of which K_u are useful subcarriers (excluding guard bands and the DC subcarrier). The users are allocated nonoverlapping subcarriers in the spectrum depending on their needs. A cyclic prefix (CP) of length L_{cp} is added to the time-domain vector. The resulting

---

Fig. 1. Discrete time baseband equivalent of an OFDMA system with M users.

block of length $K + L_{cp}$ is transmitted over the wireless channel. The symbol duration is denoted by $T_s = (K + L_{cp})T$.

The baseband channel consists of L multipath components and has the form [25, pp. 758–769]

$$h(\tau, t) = \sum_{l=0}^{L-1} h_l(t)\delta(\tau - \tau_l(t)) \tag{1}$$

where $h_l(t)$ represents the gain and $\tau_l(t)$ represents the delay of the lth path at time t. The channel impulse response $h(\tau, t)$ is modeled as a zero mean complex Gaussian process with paths being uncorrelated. Each path fades independently according to Jakes' power spectrum [31] with time-correlation function $E[h_k(t)h_k^*(t')] = \sigma_k^2 J_0(2\pi f_d(t - t'))$ where σ_k^2 is the variance of the kth path and $J_0(.)$ is the zeroth order Bessel function of the first kind, f_d is Doppler frequency in Hz. The frequency response of the channel is given by

$$H(f, t) = \sum_{l=0}^{L-1} h_l(t)\exp(-\jmath 2\pi\tau_l(t)f). \tag{2}$$

The channel frequency response vector at nth OFDM symbol is

$$\mathbf{H}_n = \mathbf{F}\mathbf{h}_n \tag{3}$$

where $\mathbf{H}_n = [H_0(n), H_1(n), \ldots, H_{K-1}(n)]^T$ with $H_k(n) = H(f = (k/KT), t = nT_s)$ representing the channel frequency response on the kth subcarrier of the nth symbol, $\mathbf{h}_n = [h_0(n), \ldots, h_{L-1}(n)]^T$ with $h_l(n) = h_l(t = nT_s)$ representing the channel gain of lth path of the nth symbol, and $\mathbf{F}$ is the sampled Fourier transform matrix with (p, q)th element given by

$$[\mathbf{F}]_{k,l} = \exp\left(\frac{-\jmath 2\pi k\tau_l}{KT}\right),$$
$$\text{for} \quad k = 0, 1, \ldots, K-1 \; l = 0, 1, \ldots, L-1. \tag{4}$$

In practice, the multipath delays can be considered to be constant over N OFDM symbols provided the variation in the multipath delays over N OFDM symbols is smaller than the temporal resolution of the system. For the system parameters considered in our work, we can assume the delay locations to be constant for $N \leq 600$ (for details refer to [16, sec. 3]).

---

[1]Even though the pilot allocation within a tile is fixed, since the tiles are located randomly in the time-frequency grid the overall pilot allocation becomes irregular (i.e., the pilot subcarriers belonging to a user, are no more uniformly spaced in an OFDM symbol).
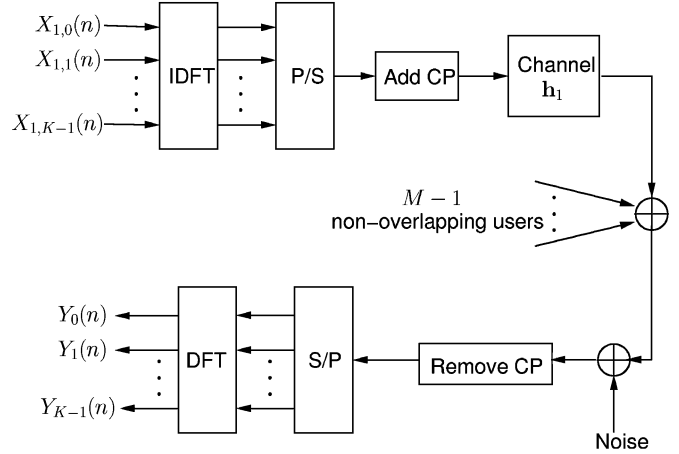
The received signal at the base-station (BS) is the sum of signals from all M users. From the received block, the CP is removed and the time-domain vector is converted to a frequency-domain vector where the users are orthogonal. Assuming the maximum delay spread of M channels is upper bounded by the duration cyclic prefix, $L_{cp}T$, and also assuming accurate synchronization at the receiver, the received signal in the frequency domain is written as

$$\mathbf{Y}_n = \sum_{i=1}^{M} \mathbf{X}_{i,n}\mathbf{H}_{i,n} + \mathbf{V}_n \qquad (5)$$

where $\mathbf{Y}_n$ is the received vector at the nth symbol, $\mathbf{X}_{i,n} = \mathrm{diag}(X_{i,0}(n), \ldots, X_{i,K-1}(n))$ is the $K \times K$ diagonal matrix with $X_{i,k}(n)$ indicating the data symbol on the kth subcarrier of the nth symbol corresponding to the ith user, and $\mathbf{H}_{i,n} = [H_{i,0}(n), \ldots, H_{i,K-1}(n)]^T$ is the $K \times 1$ vector with $H_{i,k}(n)$ indicating the channel frequency response on the kth subcarrier of the nth symbol corresponding to the ith user. The noise vector $\mathbf{V}$ is distributed as $\mathbf{V} \sim \mathcal{CN}(0, \sigma^2 \mathbf{I}_K)$. In writing (5) we have assumed that the channel gains to be constant over an OFDM symbol duration which entails neglecting inter carrier interference (ICI) due to the Doppler shift. For the simulation parameters considered in this paper, the quasi-static assumption of the channel gains holds true if the signal to noise ratio is <30 dB [18]. In further discussions, we assume the first user to be the desired user and drop the user specific subscripts.

In the signal model specified by (5), we consider the OFDM system with guard tones, and hence we do not explicitly consider pulse shaping at the transmitter or any filtering at receiver [3, sec. 8.4.2]. Moreover, as long as the transmit and receive filtering operations are not frequency selective within the bandwidth of interest, the model considered in (5) is valid [15, sec. 2].

In this paper, we consider an OFDMA system operating in partially used sub-channeling (PUSC) mode akin to the IEEE 802.16d/e WMAN project [3], [4]. The OFDM frame structure is briefly described here. The n_s consecutive OFDM symbols in time form a "slot". We reference the OFDM symbols in the qth slot as $q_1, \ldots, q_{n_s}$. The useful subcarriers of a slot are divided into the "tiles" where a tile is defined as a band of K_s frequency subcarriers by n_s time symbols, containing K_t pilots. The allocation of tiles to the users is as follows: The total bandwidth over n_t OFDM symbols is divided into n_g groups. From each group a tile is selected at random to form a "sub-channel." An user is allocated sub-channels depending on the needs. Here, we have considered the tile structure and its allocation as in IEEE 802.16d/e [3, sec. 8.4.6.2]. The uplink tile structure is as shown in Fig. 2 with $K_s = 4$, $K_t = 4$, $n_s = 3$ and pilot spacing in a tile is $t_s = 3$. The total bandwidth over $n_s = 3$ symbols is divided into $n_g = 6$ groups and a tile selected from each group form a sub-channel. In qth slot, the symbols q_1, q_3 are termed as pilot-data symbols and the symbol q_2 is termed as data-only symbol. Let N_s be the number of sub-channels allocated for the desired user in a slot. We assume that the sub-channel allocation does not change over the duration of multipath delay estimation. Let K_d be the number of subcarriers allocated to the desired user with $\mathcal{I}$ representing the corresponding subcarrier indices. The number of pilot subcarriers allocated for the de-
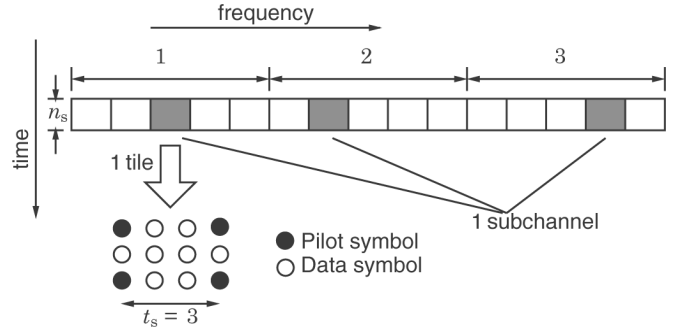

Fig. 2. Uplink OFDMA frame structure with $n_g = 3$, $n_s = 3$, $K_s = 4$, $K_t = 4$.

sired user in an OFDM symbol (first or third symbol in a slot) is $K_p = N_s \times 6 \times 2$ (this follows from tile structure given in Fig. 2). Let $\mathcal{I}_p$ represent the set of all pilot subcarrier indices of the desired user in an OFDM symbol.

We address channel estimation applied to the uplink transmission scenario described above, where the channel estimates are derived from pilots embedded in the transmission sequence. The tile structure shown in Fig. 2 will serve as the basis for this discussion. While intra-tile linear interpolation is a natural choice in this case, as the pilots "surround" the data carriers in both frequency and time dimensions, it suffers from an inherent interpolation error floor, which becomes acute in high rms-delay spread channels. Inter-tile processing which is able to use all the pilot subcarriers generated by the user has the potential to significantly minimize this error floor.

The proposed channel estimator exploits the structure of the tile as a sensor "doublet" (taken from the terminology of [22]) to estimate the multipath delays. After estimating the tap locations on the timescale within a certain error range, the algorithm localize the tap locations and finally compute the amplitude at these tap locations. It should be mentioned that the proposed channel estimation algorithm can be applied to any tile-based OFDMA system where the pilot locations in each tile form atleast a doublet structure.

III. CHANNEL ESTIMATION

After fast Fourier transform (FFT), the received signal on the pilot subcarriers (denoted by subscript "p") of the desired user is written as

$$\mathbf{Y}_{p,n} = \mathbf{X}_{p,n}\mathbf{H}_{p,n} + \mathbf{V}_{p,n} \qquad (6)$$

where $\mathbf{Y}_{p,n}$ is a $K_p \times 1$ vector representing the measurement vector as in (5) corresponding to the pilot subcarrier positions $\mathcal{I}_p$.

With the linear, Gaussian, measurement model in (6), all linear unbiased channel estimators lead to the least squares (LS) estimator [11], [26] given by

$$\hat{\mathbf{H}}_{p,n} = \mathbf{X}_{p,n}^{-1}\mathbf{Y}_{p,n} = \mathbf{H}_{p,n} + \underbrace{\mathbf{X}_{p,n}^{-1}\mathbf{V}_{p,n}}_{\mathbf{W}_{p,n}}. \qquad (7)$$

From (3) and (7) we have

$$\hat{\mathbf{H}}_{p,n} = \mathbf{F}_p\mathbf{h}_n + \mathbf{W}_{p,n} \qquad (8)$$

where $\mathbf{F}_\mathrm{p}$ is the modified $\mathbf{F}$ matrix (4) with rows corresponding to pilot indices $\mathcal{I}_\mathrm{p}$ and the noise vector is distributed as $\mathbf{W}_\mathrm{p} \sim \mathcal{CN}(0, \sigma^2 \mathbf{I}_{K_p})$ (The pilot symbols are assumed to be BPSK modulated with $|X_{\mathrm{p},n}|^2 = 1$). Equation (8) can be viewed as the output of a sensor array with L distant narrow-band sources [22]. The problem of multipath delay estimation using (8) is equivalent to direction of arrival (DOA) estimation of different narrow band sources.

The parametric channel estimation method discussed here exploits the shift invariance structure of the signal space spanned by the channel estimates corresponding to the even and odd entries of $\widehat{\mathbf{H}}_{\mathrm{p},n}$ and hence enabling the use of ESPRIT-based multipath delay estimator. The main idea involving multipath delay estimation is explained below.

A. Exposing the Shift-Invariant Structure

The elements of the vector $\widehat{\mathbf{H}}_{\mathrm{p},n}$ are rearranged to give the ordered $\widehat{\mathbf{H}}_{\mathrm{ord},n}$ as follows:

$$\widehat{\mathbf{H}}_{\mathrm{ord},n} = \begin{bmatrix} \widehat{\mathbf{H}}_{\mathrm{o},n} \\ \widehat{\mathbf{H}}_{\mathrm{e},n} \end{bmatrix} = \mathbf{H}_{\mathrm{ord},n} + \mathbf{W}_{\mathrm{ord},n} \qquad (9)$$

where $\widehat{\mathbf{H}}_{\mathrm{o},n}$, $\widehat{\mathbf{H}}_{\mathrm{e},n}$ represent the odd and even elements of the vector $\widehat{\mathbf{H}}_{\mathrm{p},n}$ respectively, and $\mathbf{W}_{\mathrm{ord},n}$ represent the corresponding rearrangement in the noise vector $\mathbf{W}_{\mathrm{p},n}$. The vectors $\widehat{\mathbf{H}}_{\mathrm{o},n}$, $\widehat{\mathbf{H}}_{\mathrm{e},n}$ are derived as

$$\widehat{\mathbf{H}}_{\mathrm{o},n} = \mathbf{J}_1 \widehat{\mathbf{H}}_{\mathrm{p},n} \quad \text{and} \quad \widehat{\mathbf{H}}_{\mathrm{e},n} = \mathbf{J}_2 \widehat{\mathbf{H}}_{\mathrm{p},n} \qquad (10)$$

where $\mathbf{J}_1$ and $\mathbf{J}_2$ are $(K_\mathrm{p}/2) \times K_\mathrm{p}$ selection matrices defined as

$$\mathbf{J}_1 = \begin{bmatrix} \mathbf{e}_1 \, \mathbf{0} \, \mathbf{e}_2 \, \mathbf{0} \, \ldots \, \mathbf{e}_{\frac{K_\mathrm{p}}{2}} \, \mathbf{0} \end{bmatrix} \qquad (11)$$

$$\mathbf{J}_2 = \begin{bmatrix} \mathbf{0} \, \mathbf{e}_1 \, \mathbf{0} \, \mathbf{e}_2 \, \ldots \, \mathbf{0} \, \mathbf{e}_{\frac{K_\mathrm{p}}{2}} \end{bmatrix}. \qquad (12)$$

We can write (10) as

$$\widehat{\mathbf{H}}_{\mathrm{ord},n} = \begin{bmatrix} \mathbf{J}_1 \widehat{\mathbf{H}}_{\mathrm{p},n} \\ \mathbf{J}_2 \widehat{\mathbf{H}}_{\mathrm{p},n} \end{bmatrix} = \begin{bmatrix} \mathbf{J}_1 \mathbf{F}_\mathrm{p} \mathbf{h}_n \\ \mathbf{J}_2 \mathbf{F}_\mathrm{p} \mathbf{h}_n \end{bmatrix} + \mathbf{W}_{\mathrm{ord},n} \qquad (13)$$

$$= \begin{bmatrix} \mathbf{F}_\mathrm{o} \\ \mathbf{F}_\mathrm{e} \end{bmatrix} \mathbf{h}_n + \mathbf{W}_{\mathrm{ord},n} \qquad (14)$$

where the two sub-matrices $\mathbf{F}_\mathrm{o}$, $\mathbf{F}_\mathrm{e}$ contain the odd and even rows of $\mathbf{F}_\mathrm{p}$, respectively. Due to the tile structure (Fig. 2) the sub-matrices are connected by a diagonal matrix

$$\Phi = \mathrm{diag} \left[\exp\left(\frac{-j2\pi t_\mathrm{s} \tau_0}{KT} \right), \ldots, \exp\left(\frac{-j2\pi t_\mathrm{s} \tau_{L-1}}{KT} \right) \right] \qquad (15)$$

as follows:

$$\mathbf{F}_\mathrm{e} = \mathbf{F}_\mathrm{o} \Phi \qquad (16)$$

where t_s is the tile separation in number of subcarriers (it is three subcarriers in [3]). Note that Φ is unitary and its diagonal elements carry the multipath delay information.

B. Proposed ESPRIT-Based Multipath Delay Estimator

From (14) and (16) we write

$$\widehat{\mathbf{H}}_{\mathrm{ord},n} = \begin{bmatrix} \mathbf{F}_\mathrm{o} \\ \mathbf{F}_\mathrm{o} \Phi \end{bmatrix} \mathbf{h}_n + \mathbf{W}_{\mathrm{ord},n} = \overline{\mathbf{F}}_\mathrm{p} \mathbf{h}_n + \mathbf{W}_{\mathrm{ord},n} \qquad (17)$$

where $\overline{\mathbf{F}}_\mathrm{p} = [\mathbf{F}_\mathrm{o} \, \mathbf{F}_\mathrm{o}\Phi]^T$. The structure of $\overline{\mathbf{F}}_\mathrm{p}$ is exploited in obtaining the estimates of the diagonal elements of Φ. The auto-correlation matrix of the channel estimates in (17) is $\mathbf{R}_\mathrm{H} = E[\widehat{\mathbf{H}}_{\mathrm{ord}} \widehat{\mathbf{H}}_{\mathrm{ord}}^H] = \overline{\mathbf{F}}_\mathrm{p} \mathbf{R}_\mathrm{h} \overline{\mathbf{F}}_\mathrm{p}^H + \sigma^2 \mathbf{I}_{K_\mathrm{p}}$, where $\mathbf{R}_\mathrm{h} = E[\mathbf{h}\mathbf{h}^H]$. Since the paths are assumed to be uncorrelated $\mathbf{R}_\mathrm{h}$ is a diagonal matrix. Let $\mathbf{U}$ represents the set of eigenvectors of $\mathbf{R}_\mathrm{H}$ corresponding to L dominant eigenvalues. Also, let $\mathbf{U}_\mathrm{o}$ and $\mathbf{U}_\mathrm{e}$ represent the first set of $K_\mathrm{p}/2$ rows and next set of $K_\mathrm{p}/2$ rows of $\mathbf{U}$, respectively. Since $\mathcal{S}\{\mathbf{U}\} = \mathcal{S}\{\overline{\mathbf{F}}_\mathrm{p}\}$, there exists a nonsingular matrix $\mathbf{B}$ such that $\mathbf{U} = \overline{\mathbf{F}}_\mathrm{p} \mathbf{B}$ [27, p. 273]. It follows that $\mathbf{U}_\mathrm{o} = \mathbf{F}_\mathrm{o}\mathbf{B}$ and $\mathbf{U}_\mathrm{e} = \mathbf{F}_\mathrm{e}\mathbf{B}$. Hence, we can write

$$\mathbf{U}_\mathrm{e} = \mathbf{F}_\mathrm{e}\mathbf{B} = \mathbf{F}_\mathrm{o}\Phi\mathbf{B} = \mathbf{U}_\mathrm{o}\mathbf{B}^{-1}\Phi\mathbf{B} = \mathbf{U}_\mathrm{o}\Upsilon \qquad (18)$$

where $\Upsilon = \mathbf{B}^{-1}\Phi\mathbf{B}$ and $\mathbf{B}$ is a nonsingular matrix. Since Υ and Φ are similar matrices, they share the same set of eigenvalues [27, pp. 314–315]. It follows that the eigenvalues of Υ are the diagonal elements of Φ. Observe that the solution for Υ in (18) is unique only when $(K_\mathrm{p}/2) \geq L$. The detailed implementation procedure involved in estimating multipath delays from $\widehat{\mathbf{H}}_{\mathrm{ord},n}$ is described next.

C. Subspace Learning and Delay Estimation

The first stage of the algorithm is the acquisition of the subspace spanned by the dominant eigenvectors of the auto-correlation matrix of channel vector $\widehat{\mathbf{H}}_{\mathrm{ord}}$. The auto-correlation matrix is not directly estimated. Rather, its decomposition via a delay-subspace tracker is estimated. The reason for using a tracking algorithm, instead of an averaging technique like the forward–backward and spatial smoothing approach [21] is due to the irregular spacing of the pilot subcarriers over the frequency grid. With such irregular pilot subcarrier spacing, the techniques such as [21] cannot be used. With irregular pilot spacing, the technique presented in [17] can be used improve the convergence speed of auto-correlation estimation.

1) Subspace Learning: The fast subspace tracking algorithm is adopted from [20] as follows:[2]

Initialize: L_m—the upper limit on the number of paths

$$\mathbf{Q}_0 = \begin{bmatrix} \mathbf{I}_{L_\mathrm{m}} \\ \mathbf{0}_{K_\mathrm{p}-L_\mathrm{m} \times L_\mathrm{m}} \end{bmatrix}, \ \ \mathbf{C}_0 = \mathbf{I}_{L_\mathrm{m}}, \ \ \mathbf{A}_0 = \mathbf{0}_{K_\mathrm{p} \times L_\mathrm{m}}, \ \ 0 \leq \gamma \leq 1. \qquad (19)$$

For pilot-data symbols update

$$\mathbf{Z}_n = \mathbf{Q}_{n-1}^H \widehat{\mathbf{H}}_{\mathrm{ord},n}, \qquad (20)$$

$$\mathbf{A}_n = \gamma \mathbf{A}_{n-1} \mathbf{C}_{n-1} + (1 - \gamma)\widehat{\mathbf{H}}_{\mathrm{ord},n} \mathbf{Z}_n^H, \qquad (21)$$

$$\mathbf{A}_n = \mathbf{Q}_n \mathbf{R}_n, \ \text{(QR decomposition)} \qquad (22)$$

$$\mathbf{C}_n = \mathbf{Q}_{n-1}^H \mathbf{Q}_n. \qquad (23)$$

The matrix $\mathbf{Q}_n$ will eventually converge to the matrix of eigenvectors of the auto-correlation matrix $\mathbf{R}_\mathrm{H} = E[\widehat{\mathbf{H}}_{\mathrm{ord}} \widehat{\mathbf{H}}_{\mathrm{ord}}^H]$. The square of the Frobenius norm of the difference between consecutive eigenvector matrices is used as a metric to quantify the convergence. Once the metric goes below

---

[2]The subspace tracking algorithm is found to be stable and computationally efficient [20].

a predefined threshold, we declare convergence. We provide the convergence plot and the choice of threshold in Section VI.

2) ESPRIT-Based Multipath Delay Estimation: Once the subspace tracking algorithm converges, the number of paths are estimated. The procedure to estimate number of paths is as follows. The eigenvalues (diagonal elements) of $\mathbf{R}_n$ are first stacked and arranged in ascending order of their magnitudes. We use generalized Akaike information criterion (GAIC) based signal length estimation technique proposed in [19] for the estimation of L. The GAIC has a cost function of the form $\mathrm{GAIC}(L) = V_L + \zeta \ln(\ln(L_{\mathrm{m}}))(L + 1)$, where ζ is the user-defined parameter. The first term V_L reflects the error for modeling the signal length to L and second is the penalty term. The penalty term ensures that over modeling is also penalized [19]. The GAIC estimate of the number of paths, $\widehat{L}$, is obtained by minimizing $\mathrm{GAIC}(L)$ with respect to L.[3] The delay subspace basis is derived as $\mathbf{Q}_{\mathrm{s}} = \mathbf{Q}_n(:, [1 : \widehat{L}])$.

The multipath delays are estimated from the delay subspace basis using the ESPRIT algorithm. The estimates of two shift invariant subspaces $\mathbf{U}_{\mathrm{o}}, \mathbf{U}_{\mathrm{e}}$ are derived from the estimated delay subspace basis as [28, pp. 1171–1175]

$$\widehat{\mathbf{U}}_{\mathrm{o}} = \begin{bmatrix} \mathbf{I}_{\frac{K_{\mathrm{P}}}{2}} & \mathbf{0}_{\frac{K_{\mathrm{P}}}{2} \times \frac{K_{\mathrm{P}}}{2}} \end{bmatrix} \mathbf{Q}_{\mathrm{s}} \qquad (24)$$

$$\widehat{\mathbf{U}}_{\mathrm{e}} = \begin{bmatrix} \mathbf{0}_{\frac{K_{\mathrm{P}}}{2} \times \frac{K_{\mathrm{P}}}{2}} & \mathbf{I}_{\frac{K_{\mathrm{P}}}{2}} \end{bmatrix} \mathbf{Q}_{\mathrm{s}} \qquad (25)$$

where the subspaces $\mathbf{U}_{\mathrm{o}}, \mathbf{U}_{\mathrm{e}}$ are such that $\mathcal{S}\{\mathbf{U}_{\mathrm{o}}\} = \mathcal{S}\{\mathbf{F}_{\mathrm{o}}\}$ and $\mathcal{S}\{\mathbf{U}_{\mathrm{e}}\} = \mathcal{S}\{\mathbf{F}_{\mathrm{e}}\}$, respectively.

The steps involved in multipath delays (tap locations) estimation are summarized as follows[28]:

(a) solve for the matrix $\widehat{\Upsilon}$, such that

$$\widehat{\mathbf{U}}_{\mathrm{o}} \widehat{\Upsilon} = \widehat{\mathbf{U}}_{\mathrm{e}} \qquad (26)$$

(b) the $\widehat{L}$ delays are estimated as (15)

$$\widehat{\tau}_i = \frac{\arg\{\lambda_i^*\} KT}{2\pi t_{\mathrm{s}}} \quad i = 0, 1, \ldots, \widehat{L} - 1 \qquad (27)$$

where $\{\lambda_i\}_{i=1}^{\hat{L}}$ are the eigenvalues of $\widehat{\Upsilon}$ and $\arg\{\lambda_i^*\}$ denotes the phase angle (in the range $[0, 2\pi)$) of λ_i^*. We assume perfect synchronization and hence $\widehat{\tau}_0 = 0$. Equation (26) can be solved by either least-squares (LS) or total least-squares (TLS) methods [22, sec. D–E] depending on the accuracy of the multipath delay estimate. Note that the angle wraps around with a period of 2π. Therefore, the maximum multipath delay that can be estimated without aliasing is KT/t_{s}. Finally, note that the multipath delays are uniquely identified if $K_{\mathrm{P}} \geq 2L$ and to avoid aliasing we require $(KT/t_{\mathrm{s}}) \geq \tau_{L-1}$.

It is important to note that since we cannot assume the pilots are evenly spaced, we cannot produce two translational invariance matrices from $\mathbf{Q}_{\mathrm{s}}$ as suggested in [15] and [17] by deleting the first row to produce $\mathbf{U}_{\mathrm{o}}$ and deleting the last row to produce $\mathbf{U}_{\mathrm{e}}$. The translational invariance can be achieved only by separating the even and odd locations representing the measurements

[3]The number of paths are estimated incorrectly only when variance of some paths (reflected in the eigenvalue of $\mathbf{R}_n$) are comparable to that of noise variance. In those cases, only the multipath delays corresponding to the dominant paths are estimated. The effect of weak multipath components on the channel frequency response is not significant.

of the first pilot in each tile, and the last pilot in each tile, respectively, separated by t_{s} subcarriers. Note that in [15] and [17], the minimum number of pilot subcarriers required to estimate of L multipath delays is $L + 1$ since the two translational invariance matrices are generated by deleting the first row and the last row of $\mathbf{Q}_{\mathrm{s}}$.

D. Channel Interpolation

In this section, we derive a channel interpolator exploiting the channel frequency correlation information defined by the multipath delays. Although the knowledge of Doppler spectrum and noise variance can be combined with multipath delay information in defining a better channel interpolator under Bayesian framework [15], we do not assume any such knowledge.

Once the multipath delays are estimated, the delay-domain channel estimates $\widetilde{\mathbf{h}}_{q_i}$ are obtained projecting the pilot channel estimates on to the basis derived from estimated multipath delays as follows:

$$\widetilde{\mathbf{h}}_{q_i} = \left(\widetilde{\mathbf{F}}_{\mathrm{p}}^H \widetilde{\mathbf{F}}_{\mathrm{p}} \right)^{-1} \widetilde{\mathbf{F}}_{\mathrm{p}}^H \widehat{\mathbf{H}}_{\mathrm{p}, q_i}, \quad i \in (1, 3) \qquad (28)$$

where $\widetilde{\mathbf{F}}_{\mathrm{p}}$ is the sampled Fourier transform matrix as in (4) with rows corresponding to pilot indices $\mathcal{I}_{\mathrm{p}}$ and columns corresponding to estimated multipath delays $\{\widehat{\tau}_i\}_{i=0}^{\widehat{L}-1}$. The channel response on the useful subcarriers of desired user is estimated as

$$\widehat{\mathbf{H}}_{q_i} = \widetilde{\mathbf{F}}_{\mathrm{d}} \widetilde{\mathbf{h}}_{q_i}, \quad i \in (1, 3) \qquad (29)$$

where $\widetilde{\mathbf{F}}_{\mathrm{d}}$ is the sampled Fourier transform matrix as in (4) with rows corresponding to user subcarrier indices $\mathcal{I}$ and columns corresponding to estimated multipath delays $\{\widehat{\tau}_i\}_{i=0}^{\widehat{L}-1}$.

The channel estimates for symbol q_2 is the simple average of the channel estimates of symbols q_1 and q_3

$$\widehat{\mathbf{H}}_{q_2} = \frac{1}{2} \left\{ \widehat{\mathbf{H}}_{q_1} + \widehat{\mathbf{H}}_{q_3} \right\}. \qquad (30)$$

Once the channel is estimated, the data subcarriers are equalized, demodulated, and then decoded.

E. Practical Considerations

The accuracy of multipath delays obtained from (27) improves with the autocorrelation averaging. Since in practice the estimation of the estimation of autocorrelation matrix involves averaging over few tens of OFDM symbols, the estimated multipath delays are inaccurate. Hence, the use of multipath delays obtained from (27) with finite averaging in channel interpolation results in performance degradation as shown in Fig. 5.

In this section, we propose a two-stage error handling procedure to increase the accuracy of the multipath delay estimate and greatly improve the system performance. The first stage involves detecting the strongest path in the vicinity of the rough estimate. In the second stage, we add few paths around the strongest to account for the smeared channel response due to nonsample spaced nature of the channel.

In order to find the strongest path, we set the error margin around each estimated delay and construct a vector of delays

$\mathbf{d}_e = \bigcup_{i=0}^{\widehat{L}-1} \mathbf{d}_i$, where $\mathbf{d}_0 = 0$, $\mathbf{d}_i = [\widehat{l}_i - \delta, \ldots, \widehat{l}_i, \ldots, \widehat{l}_i + \delta]$ and the error margin

$$\delta = \left\lfloor \nu \left(\frac{K_{\mathrm{p}}}{\widehat{L}-1} \right) \right\rfloor, \quad 0 \leq \nu \leq 0.5 \qquad (31)$$

where $\widehat{l}_i = \lceil \widehat{\tau}_i \rceil$. The δ determines the number of paths that are estimated given the set of pilot subcarriers, and ν is a user-adoptable parameter. During the qth slot, the channel gains $\widehat{\mathbf{h}}_{q_i}$ at the delays $\mathbf{d}_e$ are estimated as follows:

$$\widehat{\mathbf{h}}_{q_i} = \left(\widehat{\mathbf{F}}_{\mathrm{p}}^H \widehat{\mathbf{F}}_{\mathrm{p}} \right)^{-1} \widehat{\mathbf{F}}_{\mathrm{p}}^H \widehat{\mathbf{H}}_{\mathrm{p},q_i}, \quad i \in (1,3) \qquad (32)$$

where $\widehat{\mathbf{F}}_{\mathrm{p}}$ is the modified matrix obtained from the K-point DFT matrix by selecting rows corresponding to pilot indices $\mathcal{I}_{\mathrm{p}}$ and columns corresponding to delays $\mathbf{d}_e$. The metric $\mathcal{M}$ is then calculated as

$$\mathcal{M} = \left| \frac{1}{2} \left(\widehat{\mathbf{h}}_{q_1} + \widehat{\mathbf{h}}_{q_3} \right) \right|^2. \qquad (33)$$

In the extended region around each estimated delay $\widehat{l}_i$, we take the tap location with strongest value of the metric as the improved estimate $\widetilde{l}_i$ given by[4]

$$\widetilde{l}_i = \arg \max_{-\delta \leq k \leq \delta} \left\{ \mathcal{M}(\widehat{l}_i + k) \right\}, \text{ for } 1 \leq i \leq \widehat{L} - 1 \text{ and } \widetilde{l}_0 = 0. \qquad (34)$$

The metric used here is specifically designed for a fast fading channel in which the coherence time is comparable to the symbol length. In that case, the correlation between the channel response of two symbols falls rapidly after a time-slot length. Therefore, averaging across symbols further than a slot apart, would reduce the metric value at tap locations to a value that is indistinguishable from the noise level. On the other hand, simply averaging the tap power across time would make low-power taps undistinguishable from the noise level, and would not exploit the small-range time correlation between symbols.

Setting the constant $\nu = 0.5$ pushes the error margin to the largest value even while producing a single unique solution to (32). However, due to the irregular spacing of pilot carriers in the frequency grid, the condition number of the matrix $\widehat{\mathbf{F}}_{\mathrm{p}}$ increases with the addition of columns (corresponding to the paths). This enhances the noise effects in $\widehat{\mathbf{h}}_{q_i}$ and results in erroneous $\widetilde{l}_i$. Setting $\nu = 0$ pushes the error margin to zero which implies that there is no error in the estimated multipath delays. It is preferred to choose ν as a function of signal-to-noise ratio (SNR) since we expect the error in multipath delay estimate to reduce with an increase in SNR.

Once the strong path locations $(\widetilde{l}_i)$ in the vicinity of the path delays $(\widehat{\tau}_i)$ are estimated, we consider ε delays around each $\widetilde{l}_i$ to account for smearing effects due to nonsample spaced nature of the channel [11, Fig. 2]. With the inclusion of these extra delays, the set of delays to be used for channel interpolation takes the form $\mathbf{d} = \bigcup_{i=0}^{\widehat{L}-1} \mathbf{d}_i$, where $\mathbf{d}_0 = 0$, $\mathbf{d}_i = $

---

[4]When the estimated multipath delays $\widehat{\tau}_i$ and $\widehat{\tau}_j$ are such that $|\widehat{l}_i - \widehat{l}_j| < \delta$, we set $\widetilde{l}_i = \widehat{l}_i$ and $\widetilde{l}_j = \widehat{l}_j$. Further, when $\widehat{\tau}_i$ and $\widehat{\tau}_j$ are such that $\widehat{l}_i = \widehat{l}_j$, then we define error margin only for $\widehat{l}_i$.

$[\widetilde{l}_l - \varepsilon, \ldots, \widetilde{l}_i, \ldots, \widetilde{l}_i + \varepsilon]$ and ε is the user-defined parameter. The variable ε accounts for the smearing in the channel energy from the actual tap location to the neighboring taps. With the set $\mathbf{d}$ representing the multipath delay locations, the channel frequency response on useful subcarriers of the desired user are estimated from (28), (29), and (30).

IV. BEP ANALYSIS

In this section, we measure the performance of both inter-tile and intra-tile based channel estimation methods by evaluating uncoded bit-error probability (BEP) for uplink tile structure as proposed in [3] given by Fig. 2. The effect of channel estimation error on the BEP performance of OFDM systems in Rayleigh fading channels has been analyzed in [23]. This analysis in [23] yields a closed form BEP expression for constellation mapping with Gray coding for receivers employing a zero-forcing equalizer.

The channel estimate on a data subcarrier (for any symbol index n and subcarrier index k) is derived as

$$\widehat{H} = \mathbf{a}^H \widehat{\mathbf{H}}_{\mathrm{p}} \qquad (35)$$

where $\mathbf{a}$ is the linear combiner and $\widehat{\mathbf{H}}_{\mathrm{p}}$ is the pilot channel estimates as in (8). The expression for BEP involves statistics of the channel estimate $\widehat{H}$ and the true channel response H on the data subcarrier. Define

$$\sigma_{\mathrm{H}}^2 \triangleq \frac{1}{2} E\left[|H|^2 \right], \quad \sigma_{\widehat{\mathrm{H}}}^2 \triangleq \frac{1}{2} E\left[|\widehat{H}|^2 \right] \qquad (36)$$

where $E[|H|^2]$ and $E[|\widehat{H}|^2]$ represent the variance of the actual and estimated channel, respectively. The cross-correlation between actual and estimated channel and the correlation coefficients are defined as

$$\mu_1 + \jmath\mu_2 \triangleq E[\widehat{H}H^*], \qquad (37)$$

$$\kappa_1 \triangleq \frac{\mu_1}{\sigma_{\mathrm{H}}\sigma_{\widehat{\mathrm{H}}}}, \quad \kappa_2 \triangleq \frac{\mu_2}{\sigma_{\mathrm{H}}\sigma_{\widehat{\mathrm{H}}}}. \qquad (38)$$

The average SNR per subcarrier is defined as

$$\eta \triangleq \frac{E\left[|H|^2\right] E\left[|X|^2\right]}{E\left[|V|^2\right]}. \qquad (39)$$

Following the approach in [23], the closed form expression for bit-error rate (BER) (with QPSK modulation) is given by

$$P_b = \frac{1}{2} \left[1 - \frac{1}{2} \frac{\frac{(\kappa_1 + \kappa_2)}{\sqrt{2}}}{\sqrt{1 + \frac{1}{\eta} - \frac{(\kappa_1 - \kappa_2)^2}{2}}} - \frac{1}{2} \frac{\frac{(\kappa_1 - \kappa_2)}{\sqrt{2}}}{\sqrt{1 + \frac{1}{\eta} - \frac{(\kappa_1 + \kappa_2)^2}{2}}} \right]. \qquad (40)$$

In further discussions, we drop the time-dependent subscript n from the pilot channel estimates, since only an asymptotic BER analysis is provided.

A. BEP for Inter-Tile Based Method

In this section, we derive BEP expression for the proposed inter-tile based channel estimator. It is clear from (29) and (30) the variance of channel estimation error is different for pilot-data symbols (q_1, q_3) and data-only symbol (q_2). Hence, we separately evaluate the BEP for pilot-data symbols and

data-only symbols and weigh them accordingly to find the overall BEP. The following BEP analysis assumes actual delay locations.

Considering a pilot-data symbol of the qth slot, the channel estimate on kth data subcarrier is given by (29)

$$\widehat{H}_k = \mathbf{a}_k^H \widehat{\mathbf{H}}_{\mathrm{p}} \tag{41}$$

where $\mathbf{a}_k^H$ is the kth row of $\mathbf{F}_{\mathrm{d}}(\mathbf{F}_{\mathrm{p}}^H \mathbf{F}_{\mathrm{p}})^{-1}\mathbf{F}_{\mathrm{p}}^H$ i.e.,

$$\mathbf{a}_k^H = \mathbf{e}_k^T \mathbf{F}_{\mathrm{d}} \left(\mathbf{F}_{\mathrm{p}}^H \mathbf{F}_{\mathrm{p}}\right)^{-1} \mathbf{F}_{\mathrm{p}}^H \tag{42}$$

and $\widehat{\mathbf{H}}_{\mathrm{p}}$ is $K_{\mathrm{p}} \times 1$ vector of pilot channel estimates as in (8), $\mathbf{F}_{\mathrm{d}}$ is the sampled Fourier transform matrix as in (4) with rows corresponding to user subcarrier indices $\mathcal{I}$ and columns corresponding to actual multipath delays.

For the given linear combiner, we evaluate the statistics as (see Appendix A-1)

$$\sigma_{\mathrm{H},k}^2 = \frac{1}{2} \sum_{l=0}^{L-1} \sigma_l^2, \tag{43}$$

$$\sigma_{\widehat{\mathrm{H}},k}^2 = \frac{1}{2} \left(\sum_{l=0}^{L-1} \sigma_l^2 + \sigma^2 \mathbf{a}_k^H \mathbf{a}_k\right), \tag{44}$$

$$\mu_{1,k} = \frac{1}{2} \sum_{l=0}^{L-1} \sigma_l^2 \text{ and } \mu_{2,k} = 0. \tag{45}$$

Substituting (43), (44), and (45) in (38), we evaluate the BEP as in (40). Let $P_{\mathrm{b}}(1)$ represent the BEP for pilot-data symbols.

Similarly, for a data-only symbol the channel estimate on kth data subcarrier is estimated by averaging the channel estimates on data-pilot symbols as in (30). Proceeding in similar manner, we evaluate the statistics as (see Appendix A-2)

$$\sigma_{\mathrm{H},k}^2 = \frac{1}{2} \sum_{l=0}^{L-1} \sigma_l^2, \tag{46}$$

$$\sigma_{\widehat{\mathrm{H}},k}^2 = \frac{1}{4} \left(\{1+\mathrm{sinc}(4\pi f_{\mathrm{d}}T)\} \sum_{l=0}^{L-1} \sigma_l^2 + \sigma^2 \mathbf{a}_k^H \mathbf{a}_k\right), \tag{47}$$

$$\mu_{1,k} = \frac{\mathrm{sinc}(2\pi f_{\mathrm{d}}T)}{2} \sum_{l=0}^{L-1} \sigma_l^2 \text{ and } \mu_{2,k} = 0. \tag{48}$$

Substituting (46), (47), (48) in (38) we evaluate the BEP as in (40). Let $P_{\mathrm{b}}(2)$ represent the BEP for data-only symbol. Note that $P_{\mathrm{b}}(1)$, $P_{\mathrm{b}}(2)$ are functions of sub-channel allocation. It is clear that for a given allocation the number of data subcarriers in pilot-data symbols and data-only symbol are same. Hence, the exact BEP is given by simple averaging of BEP's $P_{\mathrm{b}}(1)$ and $P_{\mathrm{b}}(2)$ as

$$P_{\mathrm{b}} = \frac{P_{\mathrm{b}}(1) + P_{\mathrm{b}}(2)}{2}. \tag{49}$$

B. BEP for Intra-Tile Based Method

In this section, we derive BEP expression for intra-tile based/chunk based channel estimator as proposed in [10]. The intra-tile based processing treats the pilot channel estimates in each tile independently in deriving channel over data subcarriers. Since the channel estimation is done in an independent manner from tile to tile, the BEP for the intra-tile based channel estimation method is same as the average BEP over a tile. Consider a tile as shown in Fig. 2. We reference each subcarrier in a tile by two co-ordinates (m,k) where $m \in \{1,2,3\}$ denote the symbol index and $k \in \{1,2,3,4\}$ denote the subcarrier index. Let $\widehat{\mathbf{H}}_{\mathrm{t}}$ denote the $K_{\mathrm{t}} \times 1$ vector of LS channel estimates on the pilot subcarriers of the tile. The optimum linear combiner for the kth data subcarrier of the mth OFDM symbol is derived as [30, pp. 500–507]

$$\mathbf{a}_{m,k} = \mathbf{R}_{\mathrm{t}}^{-1} \mathbf{r}_{m,k} \tag{50}$$

where

$$\mathbf{R}_{\mathrm{t}} = E\left[\widehat{\mathbf{H}}_{\mathrm{t}} \widehat{\mathbf{H}}_{\mathrm{t}}^H\right], \quad \mathbf{r}_{m,k} = E\left[\widehat{\mathbf{H}}_{\mathrm{t}} H_{m,k}^*\right] \tag{51}$$

for $m \in \{1,2,3\}$, $k \in \{1,2,3,4\}$ (excluding the pilot subcarriers indices). The expressions for $\mathbf{R}_{\mathrm{t}}$ and $\mathbf{r}_{n,k}$ are provided in Appendix A-2. Since the linear combiner defined in (50) is a function of data subcarrier index, we evaluate BEP for each data subcarrier and average them to arrive at the final BEP. The channel estimate on the kth data subcarrier on the mth OFDM symbol is derived as

$$\widehat{H}_{m,k} = \mathbf{a}_{m,k}^H \widehat{\mathbf{H}}_{\mathrm{t}}. \tag{52}$$

The required statistics are evaluated as

$$\sigma_{\mathrm{H},m,k}^2 = \frac{1}{2} \sum_{l=0}^{L-1} \sigma_l^2, \tag{53}$$

$$\sigma_{\widehat{\mathrm{H}},m,k}^2 = \frac{1}{2} \left(\mathbf{a}_{m,k}^H \mathbf{R}_{\mathrm{t}} \mathbf{a}_{m,k}\right)$$
$$= \frac{1}{2} \left(\mathbf{r}_{m,k}^H \mathbf{R}_{\mathrm{t}}^{-1} \mathbf{r}_{m,k}\right), \tag{54}$$

$$\mu_{1,m,k} + \jmath\mu_{2,m,k} = \frac{1}{2} \left(\mathbf{a}_{m,k}^H \mathbf{r}_{m,k}\right)$$
$$= \frac{1}{2} \left(\mathbf{r}_{m,k}^H \mathbf{R}_{\mathrm{t}}^{-1} \mathbf{r}_{m,k}\right). \tag{55}$$

Again, substituting (53), (54), and (55) in (38), we evaluate the BEP following (40). Let $P_{\mathrm{b}}(m,k)$ represent the BEP evaluated on the kth data subcarrier of the mth OFDM symbol of the tile (excluding the pilot subcarrier positions). Finally, the BEP for intra-tile based channel estimator is the average over eight data subcarriers in a tile given by

$$P_{\mathrm{b}} = \frac{1}{8} \sum_k \sum_m P_{\mathrm{b}}(m,k). \tag{56}$$

V. DISCUSSION

In this section, we discuss two methods in reducing the number of OFDM symbols required for the multipath delay estimation.

A. Sub-Channel and Tile Allocation Schemes

The sub-channel and tile allocation scheme favorable for the proposed channel estimation method is discussed here. The
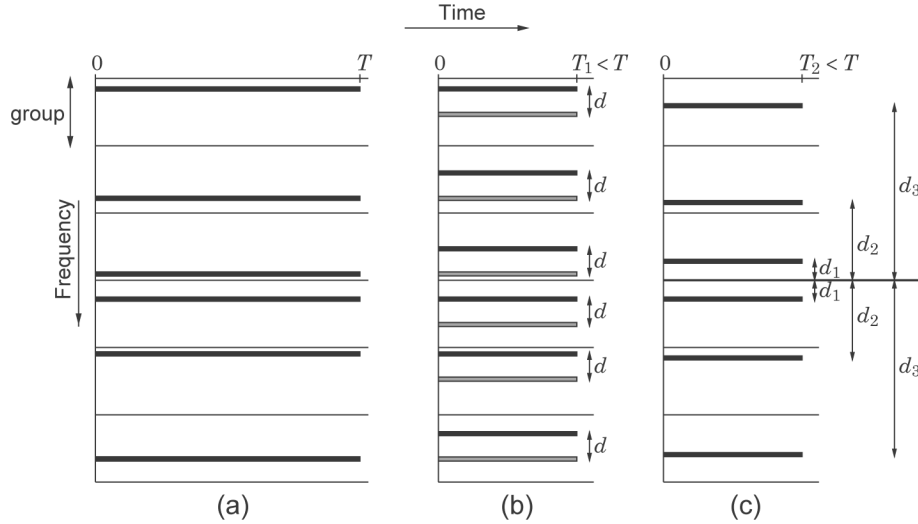
Fig. 3.   Possible tile allocation schemes. The allocation shown in (a) is adopted from IEEE 802.16d/e. The allocations shown in (b) and (c) are favorable for faster convergence compared to (a).

efficient estimation of multipath delays needs the dominant eigenvectors of $\widehat{\mathbf{R}}_{\mathrm{H}}$ reveal the correct rank corresponding to all the independent multipath components. Hence, the tile allocation should not be changed until the delay-subspace of $\widehat{\mathbf{R}}_{\mathrm{H}}$ converges to the delay-subspace of $\mathbf{R}_{\mathrm{H}}$. This allocation is represented in Fig. 3(a). Now, consider sub-channel allocation is shown in Fig. 3(b). Observe that the tiles allocated in Fig. 3(b) forms a "doublet" structure. Let $\mathcal{I}_{\mathrm{P_1}}$ and $\mathcal{I}_{\mathrm{P_2}}$ denote the pilot subcarrier indices of the 1st and 2nd member of the doublet, and let $\mathbf{F}_{\mathrm{P_1}}$ and $\mathbf{F}_{\mathrm{P_2}}$ represent the sampled Fourier transform matrices as defined in (4) with rows corresponding to pilot subcarrier indices $\mathcal{I}_{\mathrm{P_1}}$, $\mathcal{I}_{\mathrm{P_2}}$ respectively, and columns corresponding to actual multipath delays. It is clear from Fig. 3 that $\mathcal{I}_{\mathrm{P_2}} = \mathcal{I}_{\mathrm{P_1}} + d$, which allows us to write

$$\mathbf{F}_{\mathrm{P_2}} = \mathbf{F}_{\mathrm{P_1}} \Psi \qquad (57)$$

where

$$\Psi = \mathrm{diag}[\exp(-j2\pi d\tau_0/KT), \ldots, \exp(-j2\pi d\tau_{L-1}/KT)]$$

is a unitary matrix. Since the unitary transformation preserves the subspace properties, the autocorrelation matrices channel responses corresponding to $\mathcal{I}_{\mathrm{P_1}}$ and $\mathcal{I}_{\mathrm{P_2}}$ can be averaged. This averaging helps in faster convergence of the estimated delay-subspace basis and hence reduces the number of OFDM symbols required for multipath delay estimation. Observe that the minimum number of pilot subcarriers required to estimate L multipath delay locations is $K_{\mathrm{p}} = 4L$. The speed-up in the convergence is a function of channel delay-spread as discussed in [12, sec. 2.A.1].

Further, let us consider the tile allocation in a sub-channel as shown in Fig. 3(c). The tiles are allocated symmetrically around the central subcarrier. This symmetry in the tile allocation provides a centro-Hermitian structure in the signal space of the channel response on pilot subcarriers. The centro-Hermitian structure can exploited by forward–backward averaging of the

autocorrelation matrix [28, pp. 718–722]. The improved autocorrelation matrix for the tile allocation as in Fig. 3(c) is given by

$$\widehat{\mathbf{R}}_{\mathrm{H}}^{\mathrm{fb}} = \frac{\widehat{\mathbf{R}}_{\mathrm{H}} + \mathbf{J}\widehat{\mathbf{R}}_{\mathrm{H}}^{*}\mathbf{J}}{2} \qquad (58)$$

where $\mathbf{J}$ has ones on anti-diagonal elements and zeros elsewhere. Note that the minimum number of pilot subcarriers required to estimate L multipath delays remains $K_{\mathrm{p}} = 2L$.

B. Receive Diversity

The proposed method can be directly extended for systems with receive diversity. At each receiver, the channel response is independently computed even though the with power delay profile being identical across receivers [29, ch. 7]. Since the channel delay profile remains same, the estimated autocorrelation $\widehat{\mathbf{R}}_{\mathrm{H}}$ can be averaged across the receivers. Such an averaging speeds up the convergence rate of the estimated delay-subspace basis, and hence reduces the number of OFDM symbols required for multipath delay estimation.

VI. SIMULATION AND RESULTS

An OFDMA system is simulated with the following parameters: center frequency $f_{\mathrm{c}} = 3.5$ GHz; bandwidth $B = 10$ MHz; total number of subcarriers used $K = 1024$; number of useful subcarriers $K_{\mathrm{u}} = 860$; number of sub-channels allocated to the desired user per slot $N_{\mathrm{s}} = 5$; length of cyclic prefix $L_{\mathrm{cp}} = 256$; upper limit on the number of paths is taken as $L_{\mathrm{m}} = 10$; fade rate $f_{\mathrm{d}} = 200$ Hz. The user-defined parameters are set at[5] $\zeta = 6$, $\nu = 0.2$, $\varepsilon = 2$ and the forgetting factor is chosen as $\gamma = 0.995$. The multipath channel with Rayleigh coefficients is simulated with four taps with multipath delays uniformly distributed over (a) $[0 \; L_{\mathrm{cp}}T]$ (uniform power delay pro-

---

[5]We have chosen $\zeta = 6$, $\nu = 0.2$ after extensive simulations. The value for ε is chosen to accommodate maximum energy leakage, which is experienced when the fractional part of multipath delay is $0.5T$.
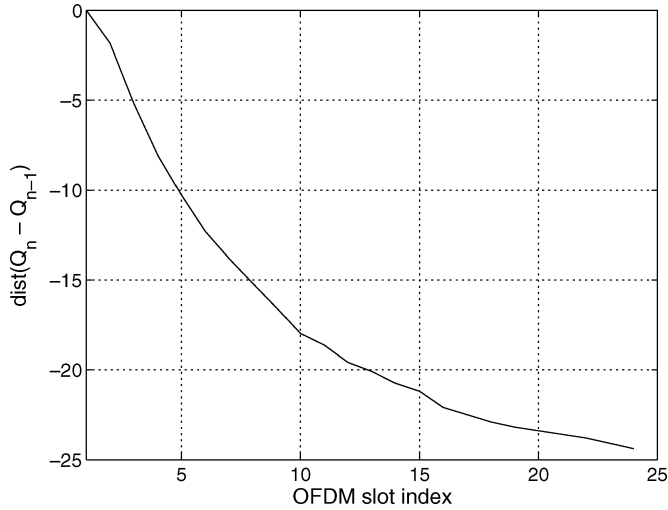
Fig. 4. Eigenvector convergence for the proposed algorithm. The measure is the distance between $\mathbf{Q}_n$ and $\mathbf{Q}_{n-1}$.
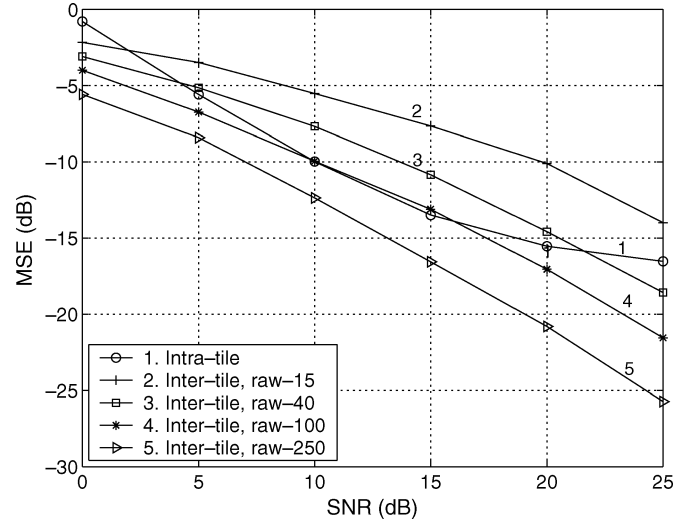

Fig. 5. MSE comparison of intra-tile and inter-tile based channel estimators for channel (c). Since only the estimated delays are used, the performance of the proposed method improves with more averaging. The performance of the curve 2 significantly improves with pre-processing on the estimated delays.

file), (b) $[0 \, (L_{\mathrm{cp}}T/2)]$ (uniform power delay profile) and (c) Vehicular-B "like" non-sample-spaced channel model:[6]

Tap index	1	2	3	4	5	6
Delay (μs)	0	0.35	8.95	12.95	17.15	20.05
Power (dB)	-2.5	0	-12.8	-10	-25.2	-16

Each path fades independently according to Jakes' power spectrum [31]. The performance of the algorithm is evaluated using total mean square error (MSE) as defined in [24] and bit error probability by averaging over different channel realizations and by independently selecting the multipath delays for the desired user. The BEP is evaluated with and without coding. The raw BEP is evaluated for Gray coded QPSK. For the coded OFDM system, the input bits are encoded with rate 3/4 parallel concatenated convolutional codes (turbo-codes) and then modulated using 16QAM as explained in [3, sec. 8.4.9].

The total MSE is defined as [24]

$$\mathrm{MSE} = \frac{1}{K_{\mathrm{d}}} \sum_{i \in \mathcal{I}} E\left\{ |H_i - \widehat{H}_i|^2 \right\}. \tag{59}$$

The intra-tile based method estimates the channel at data subcarriers using the linear interpolation method explained in Section IV-B. The convergence of the proposed algorithm is measured by square of the Frobenius norm between consecutive eigenvector matrices. The measure used to quantify the convergence is

$$\mathrm{dist}(\mathbf{Q}_n, \mathbf{Q}_{n-1}) = \frac{\mathrm{tr}\left\{ (\mathbf{Q}_n - \mathbf{Q}_{n-1})(\mathbf{Q}_n - \mathbf{Q}_{n-1})^H \right\}}{L_{\mathrm{m}}}. \tag{60}$$

Fig. 4 shows the eigenvector convergence plot at SNR = 15 dB for channel (c). The threshold for the algorithm convergence for the given SNR is set at -20 dB. It is observed from the plot that the algorithm converges in 15 OFDM slots.

Fig. 5 shows the MSE plot with inter-tile based estimator using the "raw" multipath delay estimates obtained from (27).

[6]The Vehicular-B channel is made non-sample-spaced by adding a half sample delay $0.5T = 0.05 \, \mu$s to the actual delays.

The curves labeled 2–5 are the performance curves for inter-tile based processing with *raw* delay estimates obtained by averaging the autocorrelation matrix over 15, 40, 100, and 250 OFDM slots respectively. The sub-channel allocation assumed to be constant over the autocorrelation averaging [as shown in Fig. 3(a)]. Note that the performance of the inter-tile based method improves with averaging over number of slots. It is clear from the plot that the use of multipath delays without pre-processing suffers from performance loss at practical conditions.

The simulation results provided hereafter for inter-tile based interpolation uses the pre-processed multipath delays $(\widehat{l}_i)$ obtained with averaging over 15 OFDM slots (as specified in Section III-E).

Fig. 6 shows the MSE plot comparing the inter-tile based method with the intra-tile based method for channels (a), (b) and (c). The intra-tile based method treats the channel estimates on pilots of each tile independently, while the inter-tile based method account for the frequency domain correlation between the channel estimates on pilots of different tiles in an OFDM symbol. The performance of the inter-tile based method improves with increase in SNR, whereas the intra-tile based method suffers from irreducible error floor at higher SNR. The error floor in intra-tile based method is due to its inability to exploit frequency correlation on the pilot channel estimates of different tiles. It is observed that with intra-tile processing, the MSE for channels with longer root mean square (rms) delay spread [channel (a)] floors at higher values when compared with channels with relatively smaller rms-delay spread [channel (b) and (c)]. Intra-tile based method relies on local channel information for interpolation, and hence, is sensitive to channel frequency selectivity within a tile. We have also compared the MSE performance of the proposed channel estimator with Cramer–Rao bound. The expression for the CRB is derived in Appendix B. It is observed that the proposed channel estimator is 8 dB away from CRB. The constant shift in MSE from CRB
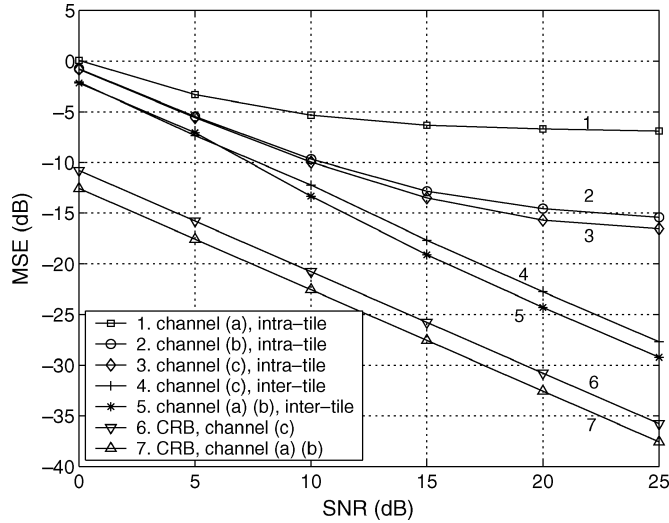
Fig. 6. MSE comparison of intra-tile and inter-tile based channel estimators for different channel models. The CRB is also plotted for comparison. The proposed inter-tile based estimator uses an extended range of $\varepsilon = 2$.
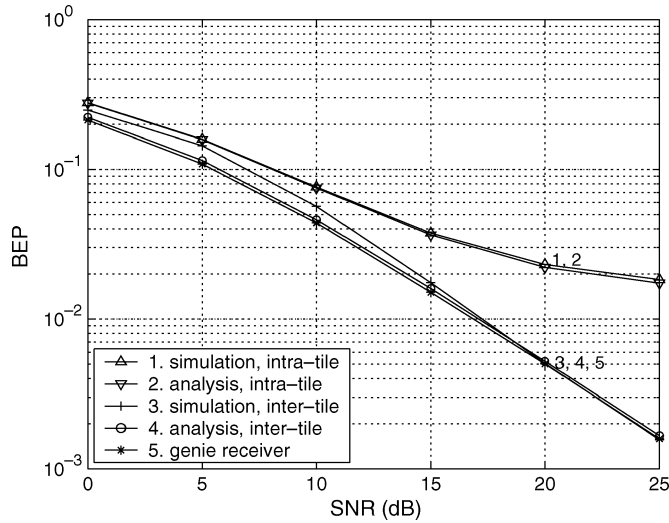

Fig. 8. Coded BEP comparison of intra-tile and inter-tile based channel estimators for channel (c). The proposed inter-tile based estimator uses an extended range of $\varepsilon = 2$.

VII. CONCLUSION

In this paper, we have described a novel channel estimation algorithm for the uplink receiver of an OFDMA system with pseudo-random tile allocation. Such pseudo-random tile allocation results in irregular and sparsely placed pilot subcarriers, which limits the use of conventional channel estimation/interpolation methods. While intra-tile channel estimation and interpolation is possible, such a method suffers from an irreducible channel estimation error floor and is also sensitive the delay-spread of the channel. The proposed inter-tile based parametric estimator exploits global channel information (frequency correlation) in defining the estimator, and hence does not exhibit any error floor over a large range of operating SNRs. This is achieved by recognizing the fact that the uplink tile structure can generate the shift invariance property in the signal space, enabling the usage of the ESPRIT algorithm to estimate the channel multipath delays. The proposed algorithm greatly reduces the pilot overheads, and is able to accurately estimate channels with large delay-spread. We are currently investigating the possibility of extending such parametric methods to the downlink, especially in the context of reuse-1 cellular OFDM systems where the co-channel interference can be considerable.

Fig. 7. Uncoded BEP comparison of intra-tile and inter-tile based channel estimators for channel (c). The proposed inter-tile based estimator uses an extended range of $\varepsilon = 2$.

is due to the finite averaging effect (over 15 slots) in estimating the delay-subspace basis vectors.

Fig. 7 shows the uncoded BEP plot for channel (c) with QPSK modulation. The performance of the proposed inter-tile based channel estimator improves with the increase in SNR and is close to the genie receiver (receiver with ideal channel knowledge). We observe that the performance of intra-tile based method exhibits error floor. Also observe that there is a close match between the simulated BEP and the analytical BEP evaluated for both inter-tile and intra-tile based channel interpolators.

Fig. 8 shows the turbo-coded BEP plot for channel (c). Where it is clear that the proposed inter-tile based method outperforms intra-tile based method. Observe that the performance of proposed algorithm is only 2 dB away from the genie receiver at a BEP of 10^{-3}.
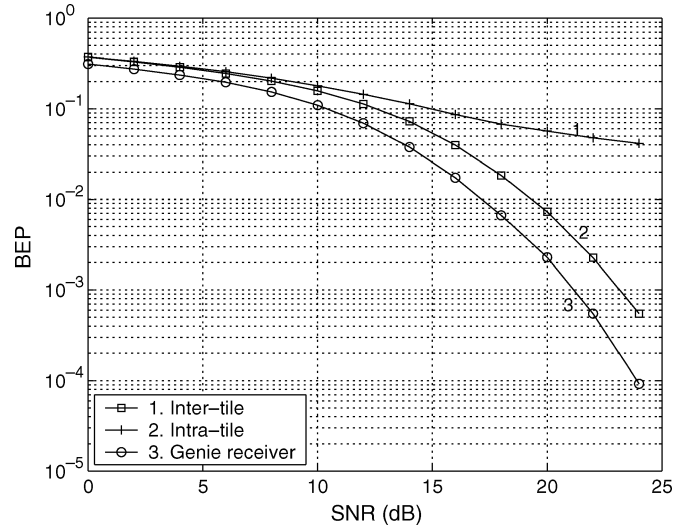
APPENDIX A

Here, we derive the required statistics (autocorrelation and cross-correlation matrices) required to evaluate BEP expression for inter-tile and intra-tile based channel estimators.

A. Statistics Required for Inter-Tile Method

For Pilot-Data Symbol: The variance of the channel on the kth subcarrier is given by

$$E\left[|H_k|^2\right] = \mathbf{f}_k^H E[\mathbf{h}\mathbf{h}^H]\mathbf{f}_k = \mathbf{f}_k^H \mathbf{R}_{\mathrm{h}}\mathbf{f}_k = \sum_{l=0}^{L-1} \sigma_l^2 \qquad (61)$$

where $\mathbf{R}_h \triangleq E[\mathbf{h}\mathbf{h}^H]$ and $\mathbf{f}_k^H$ is the kth row of $\mathbf{F}_d$, i.e., $\mathbf{f}_k^H = \mathbf{e}_k^T \mathbf{F}_d$. The variance of the estimated channel on the kth subcarrier is

$$E\left[|\widehat{H}_k|^2\right] = \mathbf{a}_k^H E\left[\widehat{\mathbf{H}}_p \widehat{\mathbf{H}}_p^H\right] \mathbf{a}_k \tag{62}$$

$$= \mathbf{a}_k^H \left(\mathbf{F}_p \mathbf{R}_h \mathbf{F}_p^H + \sigma^2 \mathbf{I}_{K_p}\right) \mathbf{a}_k \tag{63}$$

$$= \sum_{l=0}^{L-1} \sigma_l^2 + \sigma^2 \mathbf{a}_k^H \mathbf{a}_k. \tag{64}$$

The cross-correlation between the estimated channel and the actual channel on kth subcarrier is given by

$$E\left[\widehat{H}_k H_k^*\right] = \mathbf{a}_k^H E\left[\widehat{\mathbf{H}}_p H_k^*\right] \tag{65}$$

$$= \mathbf{a}_k^H \mathbf{F}_p \mathbf{R}_h \mathbf{f}_k = \sum_{l=0}^{L-1} \sigma_l^2. \tag{66}$$

For Data-Only Symbol: The channel estimates on the kth subcarrier of the data-only symbol is given as

$$\widehat{H}_k = \frac{1}{2}\left\{\widehat{H}_{q_1,k} + \widehat{H}_{q_{n_s},k}\right\}. \tag{67}$$

The variance of the channel on kth subcarrier is given by

$$E\left[|H_k|^2\right] = \sum_{l=0}^{L-1} \sigma_l^2. \tag{68}$$

The variance of the estimated channel on kth subcarrier is given by

$$E\left[|\widehat{H}_k|^2\right] = \frac{1}{4}\left(\mathbf{a}_k^H E\left[|\mathbf{H}_{p,q_1} + \mathbf{H}_{p,q_{n_s}}|^2\right] \mathbf{a}_k\right) \tag{69}$$

assuming uniform scattering function associated with Doppler frequency in simplifying the above expression we get

$$E\left[|\widehat{H}_k|^2\right] = \frac{1}{2}\left([1+\operatorname{sinc}(2\pi f_d(n_s-1)T)]\sum_{l=0}^{L-1}\sigma_l^2 + \sigma^2 \mathbf{a}_k^H \mathbf{a}_k\right). \tag{70}$$

Proceeding in a similar way, the correlation between the estimated channel and the actual channel on kth subcarrier is given by

$$E\left[\widehat{H}_k H_k^*\right] = \operatorname{sinc}(2\pi f_d T)\sum_{l=0}^{L-1}\sigma_l^2. \tag{71}$$

B. Statistics Required for Intra-Tile Based Method

The auto-correlation of pilot channel estimates over a tile is given by

$$\mathbf{R}_t = E\left[\mathbf{H}_t \mathbf{H}_t^H\right] + \mathbf{I}_{K_t}. \tag{72}$$

Since the channel time-frequency correlation information is not available at receiver, we assume uniform channel scattering function associated with a multipath delay spread of L_{cp} and a maximum Doppler frequency f_d in deriving Wiener filter coefficients [30, pp. 502-508]. The expression for $E[\mathbf{H}_t \mathbf{H}_t^H]$ is given by

$$E\left[\mathbf{H}_t \mathbf{H}_t^H\right]$$
$$= \begin{bmatrix} 1 & \beta(t_s) & \alpha(n_s) & \alpha(n_s)\beta(t_s) \\ \beta^*(t_s) & 1 & \alpha(n_s)\beta^*(t_s) & \alpha(n_s) \\ \alpha(n_s) & \alpha(n_s)\beta(t_s) & 1 & \beta(t_s) \\ \alpha(n_s)\beta^*(t_s) & \alpha(n_s) & \beta^*(t_s) & 1 \end{bmatrix} \tag{73}$$

with

$$\alpha(n) = \operatorname{sinc}(2\pi f_d(n-1)T) \quad \text{and}$$
$$\beta(k) = \operatorname{sinc}\left(\frac{\pi k L_{cp}}{K}\right)\exp\left(-\frac{j\pi k L_{cp}}{K}\right) \tag{74}$$

and the expression for $\mathbf{r}_{m,k}$ is given by

$$\mathbf{r}_{m,k} = E\left[\widehat{\mathbf{H}}_t H_{m,k}^*\right] = \begin{bmatrix} \alpha(m)\beta(k-1) \\ \alpha(m)\beta(k-K_s) \\ \alpha(m-n_s+1)\beta(k-1) \\ \alpha(m-n_s+1)\beta(k-K_s) \end{bmatrix}. \tag{75}$$

For the tile pattern considered in this paper we have the number of OFDM symbols in a slot as $n_s = 3$, number of subcarriers per tile in an OFDM symbol $K_s = 4$, pilot separation in a tile is $t_s = 3$ and the number of pilots per tile $K_t = 4$.

APPENDIX B

In this Appendix, the Cramer–Rao bound (CRB) for the channel mean squared error on the users' subcarriers is derived. Note that this bound is derived in the framework of classical estimator [26]. For the linear signal model in (6) the Fisher information matrix (FIM) is given by [26, pp. 524–531]

$$\Delta_h = \frac{\mathbf{F}_p^H \mathbf{F}_p}{\sigma^2}. \tag{76}$$

The channel mean squared error for any linear unbiased estimator is lower bounded by

$$E\left[\|\mathbf{H}_d - \widehat{\mathbf{H}}_d\|\right] \geq \operatorname{CRB}(\mathbf{H}_d) \tag{77}$$

where

$$\mathbf{H}_d = \mathbf{F}_d \mathbf{h} \tag{78}$$

and $\operatorname{CRB}(\mathbf{H}_d)$ is the CRB for the unknown vector $\mathbf{H}_d$. From the linear model in (78) the CRB for $\mathbf{H}_d$ is given by [26, pp. 45–48]

$$\operatorname{CRB}(\mathbf{H}_d) = \operatorname{tr}\left\{\mathbf{F}_d \Delta_h^{-1} \mathbf{F}_d^H\right\} \tag{79}$$

$$= \sigma^2 \operatorname{tr}\left\{\mathbf{F}_d\left(\mathbf{F}_p^H \mathbf{F}_p\right)^{-1}\mathbf{F}_d^H\right\}. \tag{80}$$

REFERENCES

[1] C. Y. Wong, R. S. Cheng, K. B. Lataief, and R. D. Murch, "Multiuser OFDM with adaptive subcarrier, bit, and power allocation," *IEEE J. Sel. Areas Commun.*, vol. 17, no. 10, pp. 1747–1758, Oct. 1999.

[2] D. Kivanc, G. Li, and H. Liu, "Computationally efficient bandwidth allocation and power control for OFDMA," *IEEE Trans. Wireless Commun.*, vol. 2, no. 6, pp. 1150–1158, Nov. 2003.

[3] *Air Interface for Fixed Broadband Wireless Access Systems*, IEEE 802.16 Standard for local and metropolitan area networks, Part 16, 2004.

[4] I. Koffman and V. Roman, "Broadband wireless access solutions based on OFDM access in IEEE 802.16," *IEEE Commun. Mag.*, vol. 40, no. 4, pp. 96–103, Apr. 2002.

[5] S. Pietrzyk, G. J. M. Janssen, R. A. N. Unit, and P. Warsaw, "Multiuser subcarrier allocation for QOS provision in the OFDMA systems," in *Proc. VTC 2002-Fall*, 2002, vol. 2, pp. 1077–1081.

[6] R. Steele, *Mobile Radio Communications*. New York: IEEE Press, 1992.

[7] M.-O. Pun, M. Morelli, and C.-C. J. Kuo, "Maximum-likelihood synchronization and channel estimation for OFDMA uplink transmissions," *IEEE Trans. Commun.*, vol. 54, no. 4, pp. 726–736, Apr. 2006.

[8] S. Sezginer and P. Bianchi, "Joint frequency offset and channel estimation in the OFDMA uplink: Cramer-Rao bounds and training sequence design," in *Proc. IEEE SPAWC*, 2005, pp. 585–589.

[9] M.-O. Pun, S.-H. Tsai, and C.-C. J. Kuo, "An EM-based joint maximum likelihood estimation of carrier frequency offset and channel for uplink OFDMA systems," in *Proc. IEEE VTC*, 2004, vol. 1, pp. 598–602.

[10] J. Bonnet and G. Auer, "Chunk-based channel estimation for uplink OFDM," in *Proc. VTC 2006-Spring*, 2006, vol. 4, pp. 1555–1559.

[11] J. J. van de Beek, O. Edfors, M. Sandell, S. K. Wilson, and P. O. Borjesson, "On channel estimation in OFDM systems," in *Proc. IEEE VTC*, Jul. 1995, vol. 2, pp. 815–819.

[12] M. R. Raghavendra and K. Giridhar, "Improving channel estimation in OFDM systems for sparse multipath channels," *IEEE Signal Process. Lett.*, vol. 12, no. 1, pp. 52–55, Jan. 2005.

[13] H. Minn and V. K. Bhargava, "An investigation into time-domain approach for OFDM channel estimation," *IEEE Trans. Broadcast.*, vol. 46, no. 4, pp. 240–248, Dec. 2000.

[14] W. Dongming, H. Bing, Z. Junhui, G. Xiqi, and Y. Xiaohu, "Channel estimation algorithms for broadband MIMO-OFDM sparse channel," in *Proc. IEEE PIMRC*, Sep. 2003, vol. 2, pp. 1929–1933.

[15] B. Yang, K. B. Letaief, R. S. Cheng, and Z. Cao, "Channel estimation for OFDM transmission in multipath fading channels based on parametric channel modeling," *IEEE Trans. Commun.*, vol. 49, no. 3, pp. 467–479, Mar. 2001.

[16] O. Simeone, Y. Bar-Ness, and U. Spagnolini, "Pilot-based channel estimation for OFDM systems by tracking the delay-subspace," *IEEE Trans. Wireless Commun.*, vol. 3, no. 1, pp. 315–325, Jan. 2004.

[17] M. R. Raghavendra, S. Bhashyam, and K. Giridhar, "Exploiting hopping pilots for parametric channel estimation in OFDM systems," *IEEE Signal Process. Lett.*, vol. 12, no. 11, pp. 737–740, Nov. 2005.

[18] Y. Li and L. J. Cimini, "Bounds on the interchannel interference of OFDM in time-varying impairments," *IEEE Trans. Commun.*, vol. 49, no. 3, pp. 401–404, Mar. 2001.

[19] H. Li, D. Liu, J. Li, and P. Stoica, "Channel order and rms delay spread estimation with application to AC power line communications," *Digital Signal Processing: A Review Journal*, vol. 13, no. 2, pp. 284–300, Apr. 2003.

[20] P. Strobach, "Low-rank adaptive filters," *IEEE Trans. Signal Process.*, vol. 44, no. 12, pp. 2932–2947, Dec. 1996.

[21] S. U. Pillai and B. H. Kwon, "Forward/backward spatial smoothing techniques for coherent signal identification," *IEEE Trans. Acoust., Speech, Signal Process.*, vol. 37, no. 1, pp. 8–15, Jan. 1989.

[22] R. Roy and T. Kailath, "ESPRIT—Estimation of signal parameters via rotational invariance techniques," *IEEE Trans. Acoust., Speech, Signal Process.*, vol. 37, no. 7, pp. 984–995, Jul. 1989.

[23] M.-X. Chang and Y. T. Su, "Performance analysis of equalized OFDM systems in Rayleigh fading," *IEEE Trans. Wireless Commun.*, vol. 1, no. 4, pp. 721–732, Oct. 2002.

[24] M. Morelli and U. Mengali, "A comparison of pilot-aided channel estimation methods for OFDM systems," *IEEE Trans. Signal Process.*, vol. 49, no. 12, pp. 3065–3073, Dec. 2001.

[25] J. G. Proakis, *Digital Communications*, 3rd ed. New York: McGraw-Hill, 1995.

[26] S. M. Kay, *Fundamentals of Statistical Signal Processing Vol. 1—Estimation Theory*. Englewood Cliffs, NJ: Prentice Hall, 1993.

[27] D. C. Lay, *Linear Algebra and Its Applications*. New York: Pearson Education, 2003.

[28] H. L. Van Trees, *Optimum Array Processing, Part 4 of Detection, Estimation, and Modulation Theory*. New York: Wiley, 2002.

[29] D. Tse and P. Viswanath, *Fundamentals of Wireless Communications*. Cambridge, U.K.: Cambridge Univ. Press, 2005.

[30] L. Hanzo, M. Munster, B. J. Choi, and T. Keller, *OFDM and MC-CDMA for Broadband Multi-User Communications, WLANs and Broadcasting*. New York: Wiley-IEEE Press, 2003.

[31] W. C. Jakes, *Microwave Mobile Communications*. New York: IEEE Press, 1993.
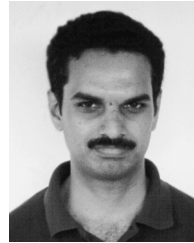
M. R. Raghavendra received the B.E. degree in telecommunications engineering from Bangalore University, Karnataka, India, in 2001. He is currently working towards the Ph.D. degree in the Department of Electrical Engineering, Indian Institute of Technology Madras, India.

His research interests cover multicarrier modulation, and signal processing for communications.

Eldar Lior received the B.Sc. degree (with honors) in computer engineering from Tel-Aviv University, Tel-Aviv, Israel, and is currently working towards the M.Sc. degree in computer science in the topic of quantum computation.

In the last three years, he has also been developing WiMAX-related algorithms in the technology industry.

Srikrishna Bhashyam received the B.Tech. degree in electronics and communication engineering from the Indian Institute of Technology, Madras, India, in 1996, and the M.S. and Ph.D. degrees in electrical and computer engineering from Rice University, Houston, TX, in 1998 and 2001, respectively.

He worked as a Senior Engineer at Qualcomm, Inc., Campbell, CA, from June 2001 to March 2003 on wideband code-division multiple access (WCDMA) modem design. Since May 2003, he has been with the Indian Institute of Technology, Madras, as an Assistant Professor in the Department of Electrical Engineering. His current research interests include wireless communications, multiple access communications, and information theory.

K. Giridhar received the B.Sc. degree in applied sciences from PSG College of Technology, Coimbatore, India, in 1985, the M.E. degree in electrical communication engineering from the Indian Institute of Science, Bangalore, in 1989, and the Ph.D. degree in electrical and computer engineering from the University of California, Santa Barbara, in 1993.

After working for a year as a research affiliate at Stanford University, Stanford, CA, he joined the Indian Institute of Technology, Madras, in 1994, where he is currently a Professor of electrical engineering. He is an active member of the TeNeT group (www.tenet.res.in), and his research interests are in the areas of adaptive estimation with a focus on MIMO-OFDM wireless transceivers, and performance analysis of wireless networks. His research group also works closely with the Center of Excellence in Wireless Technology (www.cewit.org). He is a Visiting Faculty at Sri Sathya Sai University, Prasanthi Nilayam, India.